American Mineralogist, Volume 83, pages 1353–1356, 1998

LETTERS

Structure sensitivity of pyrite oxidation: Comparison of the (100) and (111) planes

Jeffrey M. Guevremont,[1] Alicia R. Elsetinow,[1] Daniel R. Strongin,[1,*] Joakim Bebie,[2] and Martin A.A. Schoonen[2]

[1]Department of Chemistry, Temple University, Philadelphia, Pennsylvania, 19122, U.S.A.
[2]Department of Earth and Space Sciences, State University of New York, Stony Brook, New York, 11974-2100, U.S.A.

ABSTRACT

The interaction of atomically clean (100) and (111) crystallographic planes of FeS_2 with H_2O vapor, O_2, and a H_2O/O_2 mixture was investigated. A combined high pressure/ultra-high vacuum (UHV) apparatus allowed the surfaces to be reacted at environmentally relevant pressures and studied with X-ray photoelectron spectroscopy (XPS) without exposure to the atmosphere. Neither surface exhibited significant reaction in pure O_2. Exposure of FeS_2(111) to H_2O vapor resulted in significant oxidation, but under these same experimental conditions FeS_2(100) exhibited a much smaller amount of oxidation. It is suspected that on FeS_2(100), H_2O only reacted on nonstoichiometric regions (i.e., defects). Both surfaces showed substantial reaction in H_2O/O_2. The amount of FeS_2(100) and FeS_2(111) oxidation in the H_2O/O_2 mixture was more than simply the sum of the reaction observed individually in pure O_2 and H_2O. This result suggests that there is a synergy between H_2O and O_2 in oxidizing pyrite. In all cases, the amount of oxidation that occurred on FeS_2(111) was greater than on FeS_2(100). We believe that this experimental observation is due to a higher concentration of under-coordinated Fe in the outermost surface of FeS_2(111), relative to FeS_2(100).

INTRODUCTION

The structure of a surface plays a key role in determining its ability to facilitate heterogeneous chemistry. Often this dependence of reactivity on structure can be quite dramatic. The rate of ammonia formation from its elements on an Fe catalyst, for example, can vary over an order of magnitude depending on the structure of the outermost surface of that metal exposed to the reactant gas (Strongin et al. 1987). One might make the argument that the dependence of structure and reactivity for an alloy or mineral is even more complex in that different crystallographic planes of these types of materials not only expose different geometries, but also different atomic compositions. With regard to mineral chemistry, we argue here that it is important to develop the structure-reactivity relationships, because the geometric structure and atomic composition of a mineral surface is expected to play a major role in its interaction with the environment. Certainly, understanding this relationship is required for the accurate modeling of mineral surface reactivity.

Research presented here addresses the effect of surface structure on the oxidation of pyrite. Pyrite can occur in 85 different crystal forms (Dana 1903). Most natural pyrite, however, occurs in one of three crystal forms {001}, {111}, and {210} (Murowchick and Barnes 1987). Here we examine surface reactivity between the (100) and (111) crystal faces that dominate the {001} and {111} forms, respectively. Our X-ray photoelectron spectroscopy (XPS) results show that the oxidation of the outermost surface of the (111) crystallographic plane in a H_2O or H_2O/O_2 environment proceeded to a further extent than on the (100) plane.

EXPERIMENTAL METHODS

We studied (100) and (111) planes of natural pyrite from Longrono, Spain, and Turkey, respectively. Samples were typically 2 mm thick plates with areas close to ~1 cm^2. All samples used began as "as-grown" surfaces.

Experiments were conducted in an integrated ultra-high vacuum/high-pressure apparatus. In short, samples could be scrutinized with surface science techniques, transferred to a reaction cell, exposed to liquid or gas, and transferred back to UHV for further analysis. At no time during this process was the sample exposed to the ambient atmosphere.

UHV was obtained with cryogenic and turbomolecular pumps and the typical working base pressure of the UHV chamber was 6×10^{-7} Pa. X-ray photoelectron data were obtained with unmonochromatized Mg*K*α radiation (1253.6 eV) as the excitation source and double pass cylindrical mirror analyzer (CMA, pass energy of 25 eV). $2p_{3/2}$ and $2p_{1/2}$ contributions to each S 2p doublet used to fit spectra in this contribution have been constrained by a 2:1 peak area ratio, 1.8 eV separation, and 1.5 eV FWHM.

Pyrite samples were mounted on a tantalum foil and this assembly was supported by (but not fastened so that it could be removed in-situ), and in electrical contact with feed-throughs at the end of a transfer probe. Heating was achieved by passing a current through the Ta backing of the pyrite crystal. Sample temperatures were monitored with a type-K thermocouple that was spot-welded to the top edge of the sample holder.

Figure 1 depicts a schematic of the high-pressure apparatus intimately attached to the UHV chamber. Pyrite samples attached to the end of the transfer probe were withdrawn from the UHV environment into an intermediate pressure cell that was evacuated by a turbomolecular pump to 10^{-5} Pa. The transfer probe slid through Teflon seals so that the intermediate cell was never directly exposed to the UHV chamber. Once the sample was within the intermediate cell and isolated from UHV by a gate valve the pressure of this chamber was increased to 1 bar with dry nitrogen. A mechanical pincer was used to remove the sample from the end of the transfer probe and transport it to the reaction cell. After well-controlled exposure to gas (or liquid), the sample could typically be returned to the UHV environment ($<10^{-6}$ Pa) in 10–20 min.

Samples for study were prepared by a combination of ion bom-

*E-mail: dstrongi@nimbus.ocis.temple.edu

0003-004X/98/1112–1348$05.00

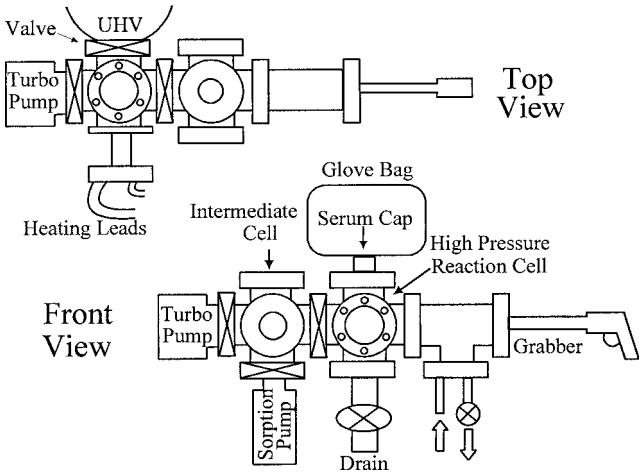

FIGURE 1. Schematic of an integrated high pressure/UHV apparatus used.

bardment in UHV and acid rinsing in the high-pressure cell. Ion bombardment of pyrite in UHV was similar to that described by Chaturvedi et al. (1996), except that 1000 eV He^+, rather than 200 eV He^+, was used to compensate for a relatively inefficient "sputtering" angle between the sample and ion gun. To remove structural damage resulting from the high energy bombardment, samples were acid rinsed (90 s exposure to 5 mL of 0.5 M HCl) in the high-pressure cell, rinsed with deoxygenated H_2O, blown dry with N_2, and returned to UHV. Comparison of S 2p and Fe 2p XPS for the acid rinsed samples to prior XPS results for cleaved pyrite (Bronold et al. 1994) is difficult due to differences in experimental conditions. Based on S 2p data it appears that a higher concentration of monosulfide impurity (see below) is present on the acid-rinsed sample, but more detailed experiments are needed for verification. Bronold et al. (1993) also present similar XPS results to ours for FeS_2(100) and FeS_2(111), after exposure to an acid environment.

Exposure to O_2 was carried out by admitting an ultra-pure grade of this gas at a pressure of 1 bar, without further treatment into the intermediate cell. Exposures involving H_2O vapor were carried out by first preparing deoxygenated H_2O following the protocol outlined by Bebie et al. (1998). Using a glass-syringe, this water was injected (through the serum cap shown in Fig. 1) into a closed "drain" at the bottom of the reaction cell. The sample was placed above the liquid and the vapor pressure of water in all our experiments was 0.023 bar. Experiments that utilized H_2O vapor alone were carried out in a 1 bar background pressure of ultra-pure N_2.

RESULTS AND DISCUSSION

Oxidation of FeS_2(100)

S 2p data (Fig. 2) for clean FeS_2(100) are fitted with two S 2p doublets, with maxima at 162.5 and 161.5 eV. Based on prior research on this crystallographic plane of pyrite, the 162.5 eV was assigned to the disulfide group and the 161.5 eV feature to a monosulfide species (Knipe et al. 1994; Nesbitt and Muir 1994; Eggleston et al. 1996). The relative integrated area of the disulfide to monosulfide doublet features was somewhat variable from crystal to crystal; the ratio being in the range of 10 to 5 (4 different samples studied). This variability in surface structure is perhaps not surprising considering that the histories of the samples are probably different. Regardless of the ratio, the fundamental behavior upon exposure to H_2O and/or O_2 was similar, and is typified by S 2p data presented in Figure 2. After a 20 h H_2O exposure, new high binding energy S 2p spectral weight appeared and grew slightly in intensity upon a continued exposure to 400 h. Based on the 400 h spectrum, we speculate that exposure to H_2O eliminated the majority of the monosulfide species and created at least two new distinct sulfur species having contributions at 163.4 and 168.8 eV, which may be associated with polysulfide and a sulfur oxide, such as sulfate (Knipe et al. 1995). Alternatively, the approximate equality of the integrated area of the 163.4 and 168.8 eV features might suggest that thiosulfate is a stable surface intermediate. For our purposes, however, the exact identity of the surface product(s) is not essential.

Exposure to O_2 resulted in some new high binding energy S 2p spectral weight near 168.5 eV, but due to its weak intensity, we

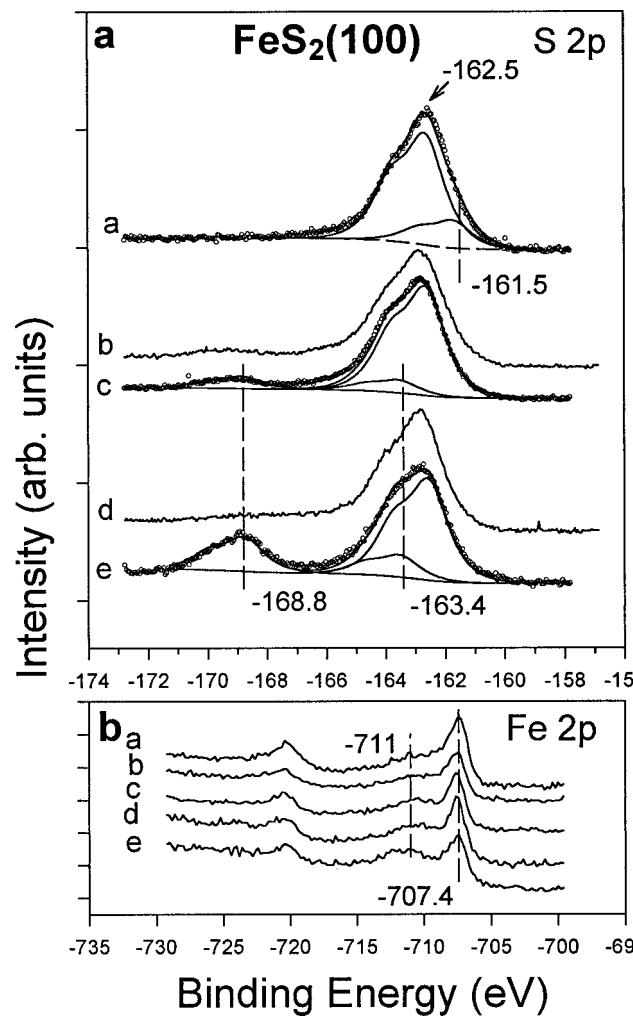

FIGURE 2. S 2p (**top**) and Fe 2p (**bottom**) data of FeS_2(100) after (**a**) acid-washing, (**b**) exposure to 20 h of H_2O vapor, (**c**) 400 h of H_2O vapor, (**d**) 20 h of O_2, and (**e**) 20 h of a H_2O vapor/O_2 mixture.

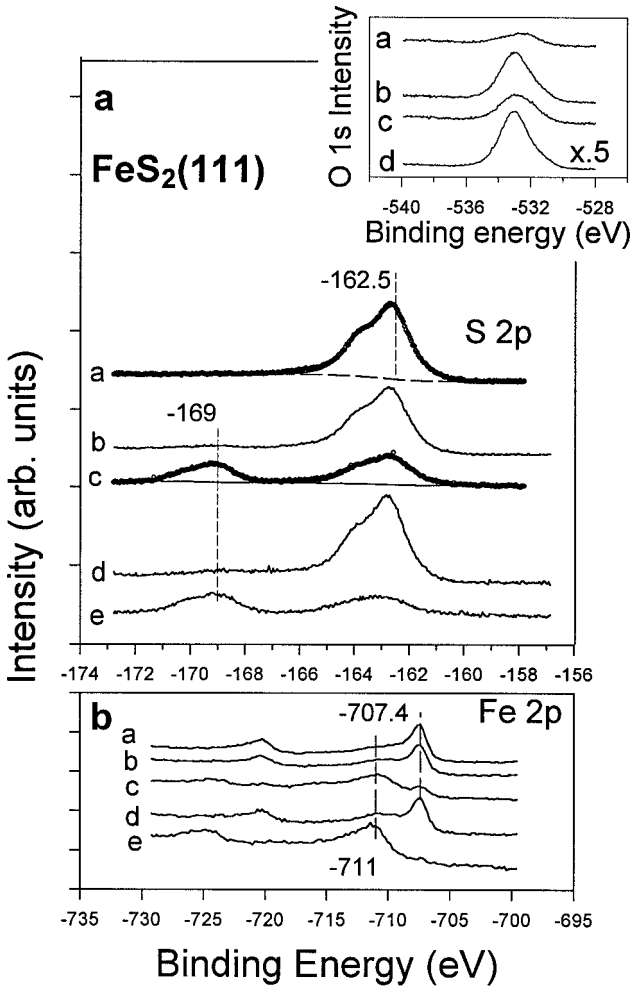

FIGURE 3. S 2p (**top**) and Fe 2p (**bottom**) data of FeS_2(111) after (**a**) acid-washing, (**b**) exposure to 20 h of H_2O vapor, (**c**) 200 h of H_2O vapor, (**d**) 20 h of O_2, and (**e**) 20 h of a H_2O vapor/O_2 mixture. The inset exhibits O 1s data for FeS_2(111) after (**a**) acid-washing, (**b**) 200 h of H_2O vapor, (**c**) 20 h of O_2, and (d) 20 h of a H_2O vapor/O_2 mixture.

refrain from making assignments except that the S^{5+} or S^{6+} oxidation state exists. Reaction of the FeS_2(100) surface in a H_2O/O_2 mixture resulted in significant S oxidation, and in that circumstance the disulfide group (contribution at 162.5 eV) was converted in part to sulfur oxide product. As before, whether the fitted peaks at 168.8 and 163.4 eV are due to sulfate, polysulfide and/or thiosulfate cannot be ascertained from these data.

The clean pyrite Fe 2p spectrum exhibits a relatively sharp feature at 707.4 eV consistent with prior research (Knipe et al. 1994; Nesbitt and Muir 1994). The broad shoulder at higher binding energy probably contains contributions from Fe^{3+} impurity as well as from Fe^{2+}. Exposure of FeS_2(100) to pure H_2O vapor or O_2 gas resulted in relatively weak spectral weight growth near 711 eV that is associated with Fe^{3+} (possibly an iron oxide and/or hydroxide). Fe 2p data after exposure to the H_2O/O_2 mixture showed an increased amount of spectral weight near 711 eV, suggesting that there was more oxidation of pyrite Fe when both O_2 and H_2O were present.

Oxidation of FeS_2(111)

S 2p data for the acid-rinsed (111) surface (Fig. 3) suggest that the concentration of monosulfide was less than on FeS_2(100), because within the resolution of our measurement, only a S 2p doublet at 162.5 eV was needed to represent the data. S 2p spectra of two additional acid-washed FeS_2(111) crystals yielded similar spectra, suggesting that this plane of FeS_2 may have an inherently smaller monosulfide contribution than FeS_2(100). Reaction of FeS_2(111) with H_2O vapor for 20 h led to a relatively small amount of high binding energy S 2p spectral weight. A 200 h exposure to H_2O vapor, however, resulted in a significant loss in the disulfide contribution and increase in S 2p spectral weight near 169 eV. It is suspected that the oxide product in this circumstance was SO_4, aside from the disulfide contribution, there was no evidence for an additional S species with a lower oxidation state [near 163.4 eV as for H_2O/FeS_2(100)]. Exposure of FeS_2(111) to a H_2O/O_2 mixture resulted in even more significant oxidation; after only 20 h the amount of oxidation was greater than that amount achieved with a 200 h pure H_2O vapor exposure.

Complementary Fe 2p data (Fig. 3, bottom) are consistent with the S 2p data. Exposure to pure H_2O for 200 h resulted in a marked reduction in the Fe 2p feature at 707.4 eV that is associated with Fe^{2+} of pyrite and increase in weight near 711 eV that is due to Fe^{3+}. This experimental observation is consistent with the loss of the 162.5 eV feature in the S 2p feature (Fig. 3, top, spectrum c) that is associated with the disulfur group of pyrite. Little change occurred in the Fe 2p spectrum after exposure to O_2, but exposure of FeS_2(111) to the H_2O/O_2 mixture resulted in the elimination of the Fe 2p feature at 707.4 eV, and the growth of a relatively intense feature at 711 eV. These latter spectral changes indicate that the near surface region of FeS_2(111) was almost completely converted to iron oxide (and/or hydroxide) and sulfur oxide.

Our assignments for oxidized iron and sulfur species are generally consistent with the experimental observation that increases in the concentrations of these products correlate with increases in oxygen surface concentration, as evidenced by O 1s data (inset to Fig. 3). Many species may contribute to the O 1s spectrum (e.g., sulfur oxide, iron oxide, iron hydroxide, etc.), and we refrain from any further analysis of these specific data, due to the expected ambiguity inherent in any interpretation.

Comparison of the oxidation behavior of the (100) and (111) planes of FeS_2

Under similar conditions, FeS_2(111) showed greater oxidation than FeS_2(100). Perhaps, the most noticeable difference was that after exposure to pure H_2O there was minimal oxidation of FeS_2(100), but a significant amount of oxidation on FeS_2(111). FeS_2(100) did exhibit substantial oxidation of both the iron and disulfide group in the H_2O/O_2 mixture environment, but the oxidative degradation of FeS_2(111) under these same experimental conditions was much more severe. For either surface, the extent of oxidation in the H_2O/O_2 mixture was far greater than what can be accounted for by simply taking the sum of the activities of each surface after individual exposure to H_2O and O_2. We do not fully understand the synergy between O_2 and H_2O, but suspect it was due the oxidation of Fe^{2+} by O_2 and the subsequent dissociation of H_2O on the resulting Fe^{3+} (Guevremont et al., unpublished manuscript).

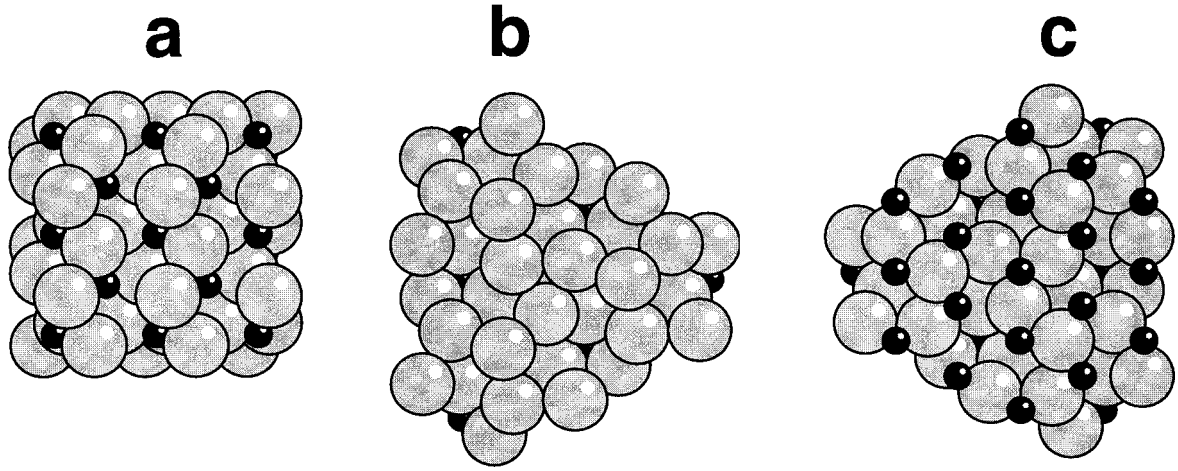

FIGURE 4. Ideal planes of FeS_2 (**a**) S-terminated (100), (**b**) S-terminated (111), and (**c**) Fe-terminated.

The structure of FeS_2(100) has been addressed by both scanning tunneling microscopy (Siebert and Stocker 1992; Eggleston and Hochella 1992) and low energy electron diffraction (Pettenkofer et al. 1991). These techniques have suggested that the (100) terrace, which was probably the portion of the surface that was analyzed in these prior studies, was close to an ideal termination. This study and photoemission research (Bronold et al. 1994) suggested that the surface was terminated by the disulfide group (Fig. 4a).

Unfortunately, the structure of FeS_2(111) has not been studied to the same extent as has the cubic face. Assuming an ideal termination of the pyrite bulk structure, the geometric structure of the surface might be expected to be approximated by the surfaces shown in Figures 4b and 4c. A (111) surface that exposes Fe in the outermost layer (Fig. 4c) would be reasonable, considering that ready access of reacting H_2O or O_2 to this site might facilitate the oxidation process. This contention is consistent with the experimental observation that some oxidation of the iron and sulfur components of FeS_2(100) occurred in pure H_2O, but it was on defect sites. Recent vacuum-based research (Guevremont et al. 1997, 1998) suggested that these defect sites consist, at least in part, of sulfur deficient sites that should expose iron sites.

More research is needed on the exact structure of the (111), and even the (100) plane of FeS_2 to bring our statements to a level higher than that of speculation. The utility of conclusions based on ideal surface structures may be limited, because surfaces often undergo a significant reconstruction, adopting a structure that is not commensurate with the bulk (Somorjai 1994). Regardless of the exact structure of the surfaces, the results reported here confirm the widely accepted notion that reaction rates on non-equivalent crystallographic orientations may differ significantly. The geological implication of these results is that the persistence of pyrite in the {111} form in aqueous systems is expected to be significantly less than for the {001} form. For experimentalists, the results imply that crushed pyrite used in batch experiments represents an ensemble of crystals with different crystallographic orientations, and, therefore, different reactivities.

ACKNOWLEDGMENTS

D.R.S. and M.A.A.S. greatly appreciates support from the Department of Energy, Basic Energy Sciences from grant DEFG0296ER14644 and DEFG029ER14633, respectively. Finally, we appreciate the critical review of Carrick Eggleston and an anonymous reviewer that significantly improved this contribution.

REFERENCES CITED

Bebie, J., Schoonen, M.A.A., Fuhrmann, M., and Strongin, D.R. (1998) Surface charge development on transition metal sulfides: an electrokinetic study. Geochimica et Cosmochimica Acta, 62(5), 633–642.

Bronold, M., Büker, K., Kubala, S., Pettenkofer, C., and Tributsch, H. (1993) Surface Preparation of FeS_2 via electrochemical etching and interface formation with metals. Physica Status Solidi, 135, 231–243.

Bronold, M., Tomm, Y., and Jaegermann, W. (1994) Surface states of cubic d-band semiconductor pyrite (FeS_2). Surface Science Letters, 314, L931–L936.

Chaturvedi, S., Katz, R., Guevremont, J., Schoonen, M.A.A., and Strongin, D.R. (1996) XPS and LEED study of a single-crystal surface of pyrite. American Mineralogist, 81, 261–264.

Dana, E.S. (1903) The system of mineralogy of James Dwight Dana. Wiley, New York.

Eggleston, C.M., Ehrhardt, J., and Stumm, W. (1996) Surface structural controls on pyrite oxidation kinetics: an XPS-UPS, STM and modeling study. American Minerologist, 81, 1036–1056.

Eggleston, C.M. and Hochella, M.F. (1992) Scanning tunneling microscopy of pyrite {100} surface structure and step reconstruction. American Mineralogist, 77, 221–224.

Guevremont, J.M., Strongin, D.R., and Schoonen, M.A.A. (1997) Effects of imperfections on the thermal chemistry of CH_3OH and H_2O on FeS_2(100): using adsorbed xenon as a probe of mineral surface structure. Surface Science, 391, 109–124.

———(1998) Photoemission of adsorbed xenon, x-ray photoelectron spectroscopy, and temperature-programmed desorption studies of H_2O on FeS_2(100). Langmuir, 14, 1361–1366.

Knipe, S.W., Mycroft, J.R., Pratt, A.R., Nesbitt, H.W., and Bancroft, G.M. (1995) X-ray photoelectron spectroscopic study of water adsorption on iron sulphide minerals. Geochimica et Cosmochimica Acta, 59, 1079–1090.

Murowchick, J.B. and Barnes, H.L. (1987) Effects of temperature and degree of supersaturation on pyrite morphology. American Mineralogist, 72, 11–12.

Nesbitt, H.W. and Muir, I.J. (1994) X-ray photoelectron spectroscopic study of a pristine pyrite surface reacted with water vapor and air. Geochimica et Cosmochimica Acta, 58(21), 4667–4679.

Pettenkofer, C., Jaegermann, W., and Bronold, M. (1991) Site specific surface interaction of electron donors and acceptors on iron disulfide (100) cleavage planes. Berichte der Bunsengesellschaft Physical Chemistry, 95(5), 560–565.

Siebert, D. and Stocker, W. (1992) Investigation of a (100) surface of pyrite by STM. Physica Status Solidi, (a) 134, K17–K20.

Somorjai, G.A. (1994) Introduction to surface chemistry and catalysis, p. 367. Wiley, New York.

Strongin, D.R., Carrazza, J., Bare, S.R., and Somorjai, G.A. (1987) The importance of C_7 sites and surface roughness in the ammonia synthesis reaction over iron. Journal of Catalysis, 103, 213.

MANUSCRIPT RECEIVED JUNE 1, 1998
MANUSCRIPT ACCEPTED JULY 28, 1998
PAPER HANDLED BY ANNE M. HOFMEISTER